

# Properties of a Highly Birefringent Photonic Crystal Fiber

J. Ju, W. Jin, *Senior Member, IEEE*, and M. S. Demokan, *Senior Member, IEEE*

**Abstract**—We report the results of our recent investigation on the properties of a highly birefringent photonic crystal fiber including modal birefringence, mode field diameter, divergence angle, and polarization mode dispersion, which are important for sensing and communication applications.

**Index Terms**—Birefringence, finite-element method (FEM), photonic crystal fiber (PCF), polarization.

## I. INTRODUCTION

PHOTONIC crystal fibers (PCFs) have attracted significant attention recently because of their unusual properties such as endlessly single-mode operation [1] and anomalous group-velocity dispersion (GVD) in the visible region [2], [3]. PCF can be made highly birefringent (HB) by having different airhole diameters along the two orthogonal axes [4], [5] or by asymmetric core design [6]. These fibers have demonstrated modal birefringence of an order of magnitude higher than that of the conventional high-birefringent fiber [7] and have potential for a number of applications such as high bit rate communication systems, polarization maintaining (PM) pigtailed photonic devices, and PM fiber loops for gyroscopes. These applications require a detailed investigation of the optical properties of PCFs, which, to our knowledge, have not been fully investigated. These properties include modal birefringence, mode field diameter, divergence angle (or numerical aperture), and polarization mode dispersion. We here report the results of our investigation on the properties of the PCF first reported by Ortigosa-Blanch *et al.* [4]

## II. RESULTS AND DISCUSSION

A full-vector finite-element method (FEM) with perfect conductor boundary conditions [8], [9] is used to perform numerical calculation. The cross section of the PCF is modeled by an idealized version with all the holes assumed to be circular and their sizes matched to that of the scanning electron micrograph (SEM) of the PCF presented in [4]. The central part of the PCF is magnified and shown in Fig. 1, and the full domain in our calculation is a circular area with a radius of  $27 \mu\text{m}$ . Before the FEM program was applied to the fiber shown in Fig. 1, it was tested with step index fibers and other PCF fiber structures. The calculated propagation constant and dispersion property agree well with the reported data in [9].

Manuscript received April 10, 2003; revised June 10, 2003.

The authors are with the Department of Electrical Engineering, the Hong Kong Polytechnic University, Hong Kong, SAR, China (e-mail: jianju.ee@polyu.edu.hk).

Digital Object Identifier 10.1109/LPT.2003.818051

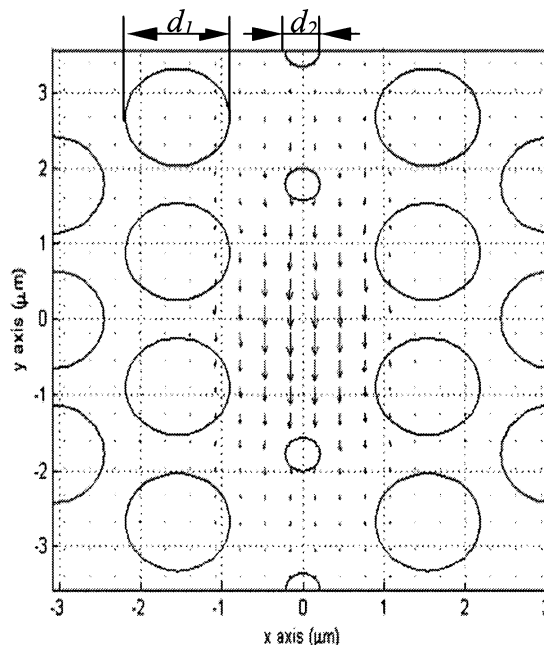


Fig. 1. Electric field vectors of the  $y$ -polarized fundamental mode.

Our calculation confirms that two nondegenerate fundamental modes are well confined to the core region. By analogy to the conventional HB fibers, we call these two approximately linearly polarized modes as  $HE_{11}^x$  and  $HE_{11}^y$ , respectively. Fig. 1 shows the electric field vector of the  $y$ -polarized fundamental mode. The effective index corresponding to the two polarization modes are denoted as  $n_x$  and  $n_y$ . The modal birefringence  $B = |n_x - n_y|$  of such a fiber as a function of wavelength is shown in Fig. 2 (the line with crosses). At wavelength  $1540 \text{ nm}$ , the birefringence is  $4 \times 10^{-3}$ , corresponding to a beat length  $L_B = \lambda/B = 0.385 \text{ mm}$ . This value is in good agreement with the measurement data ( $L_B = 0.42 \text{ mm}$ ) reported in [4].

For the HB PCF reported in [4], anisotropy was induced by positioning of capillaries with the same external diameter but different wall thickness, leading to different airhole sizes in the cladding of the PCF. The influence of hole size on the modal birefringence is, thus, important from a practical design point of view. The computer simulation results of the modal birefringence for the PCFs with various hole size are also presented in Fig. 2. As expected, the birefringence increases with a decrease in the size of the small holes ( $d_1$ ) [see Fig. 2(a)] and an increase in the ratio of the size of the big holes over the pitch  $d_2/\Lambda$  [see Fig. 2(b)]. However, increasing birefringence through reducing the size of the small holes may not be practical because

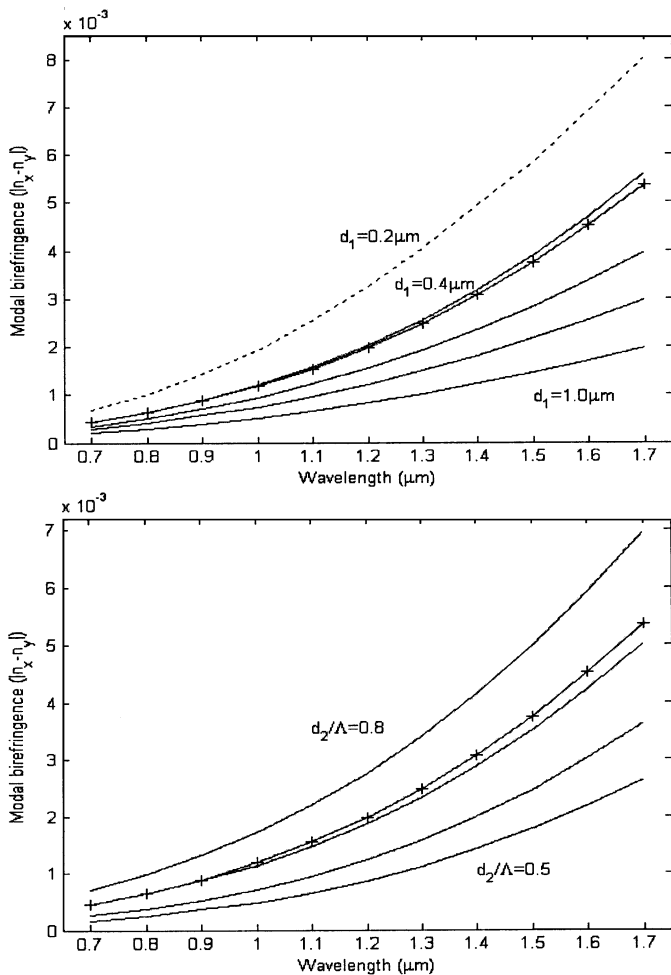


Fig. 2. Dependence of modal birefringence on the size of the holes. (a) The sizes of the small holes are increased from  $d_1 = 0.2 \mu\text{m}$  to  $1.0 \mu\text{m}$  in steps of  $0.2 \mu\text{m}$  with  $d_2/\Lambda = 0.6$ . (b) The size to pitch ratio for the big holes is increased from  $d_2/\Lambda = 0.5$  to  $0.8$  in steps of  $0.1$  with  $d_1 = 0.4 \mu\text{m}$ . The lines with crosses in them are the simulated results for the fiber presented in [4] with  $d_1 = 0.43 \mu\text{m}$ ,  $d_2 = 1.3 \mu\text{m}$  and  $\Lambda = 1.8 \mu\text{m}$ .

the light confinement property of the fiber is affected when the hole size becomes small. In our simulation, we found a large portion of light field extends beyond the first small holes for  $d_1 = 0.2 \mu\text{m}$  although a relative high birefringence can be obtained [the dotted line in Fig. 2(a)]. It is, therefore, more practical to achieve a higher birefringence through the increase in  $d_2/\Lambda$ . However, an increase in the value of  $d_2/\Lambda$  would result in multimode operation at the working wavelength. We have conducted extensive search on the possible modes that can be supported by the PCF and found that, for  $d_1 = 0.4 \mu\text{m}$  and  $d_2/\Lambda = 0.8$ , such PCF cannot support a second-order mode when the operating wavelength is beyond  $\sim 1.4 \mu\text{m}$ . Further simulation shows PCF with  $d_2/\Lambda = 0.5$  is single mode at wavelength  $1.3 \mu\text{m}$ .

The nondegeneracy of the two polarizations verified by the computed values of effective indexes can lead to different group velocity. Different group velocities caused by the small departures from perfect hexagonal symmetry have been experimentally observed [3]. The GVD, which is an important parameter for high bit-rate transmission systems that uses polarization maintaining fibers [5], was calculated and is

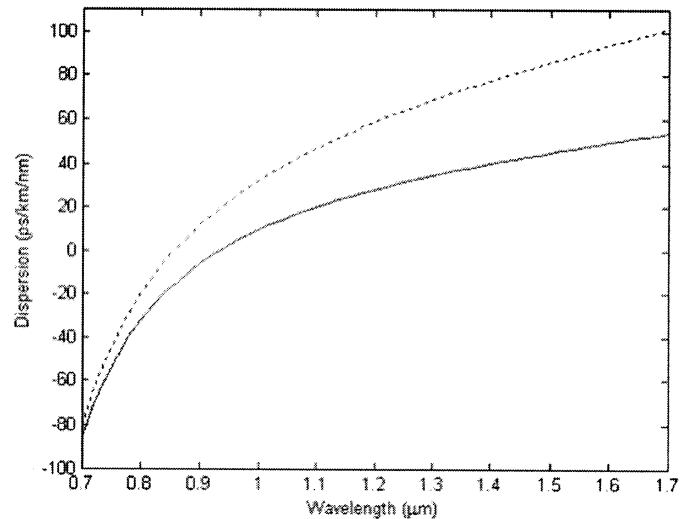


Fig. 3. Calculated GVD for the two fundamental polarization modes of the fiber presented in [4]: the  $x$  polarized (solid line) and the  $y$  polarized (dotted line).

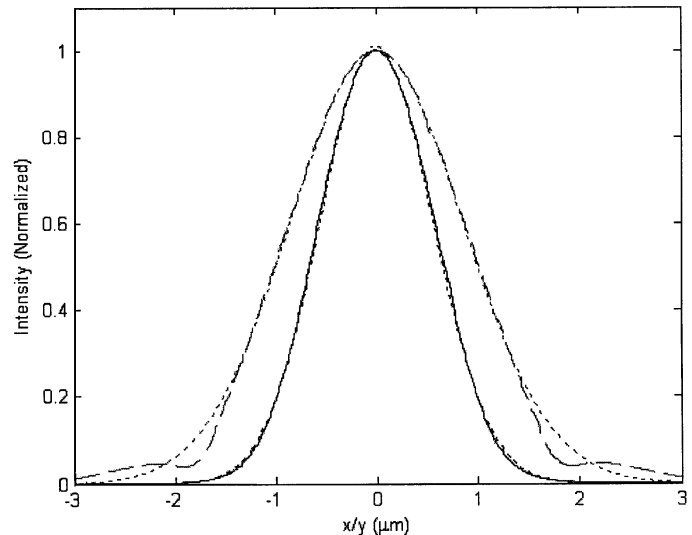


Fig. 4. Normalized intensity of  $y$ -polarized fundamental mode ( $\lambda = 1540 \text{nm}$ ,  $x$  direction: solid line;  $y$  direction: dashed line) and the corresponding Gaussian fit (dotted line).

shown in Fig. 3. The large polarization mode dispersion is an indication of the intentionally introduced anisotropy in PCF.

Mode field width  $w$  and half divergence angle  $\theta$  are important parameters for the study fiber to fiber and fiber to waveguide joints, bending induced loss, and nonlinear fiber optics. For a Gaussian field, the mode field width (diameter)  $w$  is that at which power is reduced to  $1/e^2$  of the maximum power, and the corresponding half divergence angle  $\theta$  can be expressed as  $\theta \cong \tan^{-1} \lambda/\pi w$  [10]. Since the light intensity distribution of the highly birefringent PCF is not circularly symmetric, the mode field widths ( $w_x$  and  $w_y$ ) and the half divergence angles ( $\theta_x$  and  $\theta_y$ ) along the  $x$  and  $y$  directions are different. Numerical calculation shows that the intensity distributions along the two orthogonal directions can be approximated by proper Gaussian functions (see Fig. 4), and the root mean square (rms) error of the  $x$  and  $y$  direction intensity fitting is  $0.012$  and  $0.065$  for the

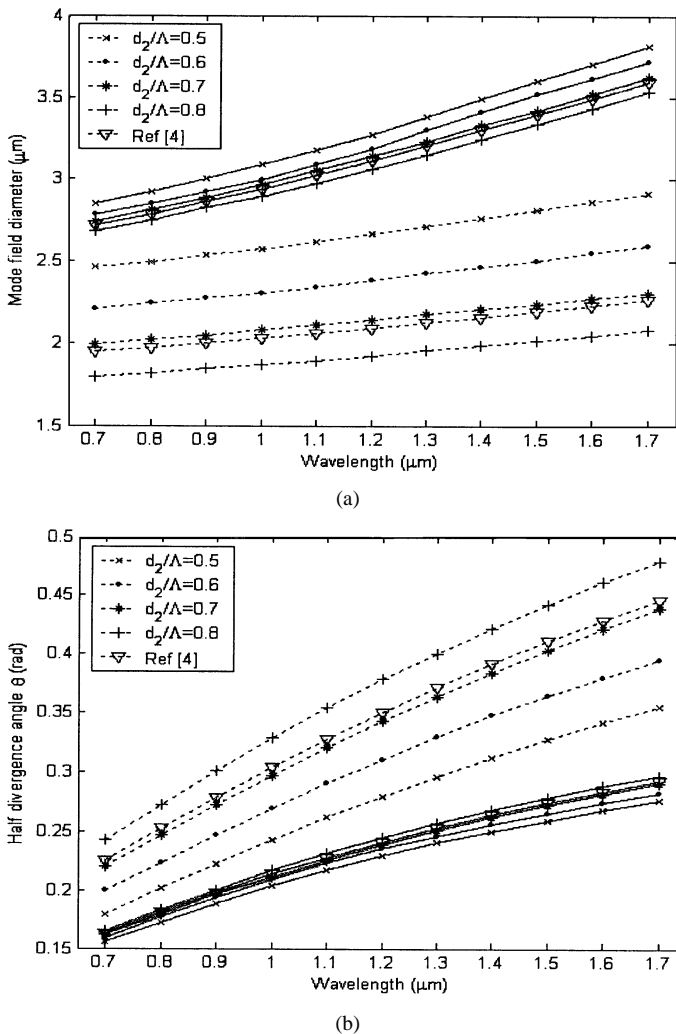


Fig. 5. (a) The mode field width ( $w_x$ : the dotted lines;  $w_y$ : the solid lines) of the  $y$ -polarized mode as function of wavelength for various  $d_2/\Lambda$ . (b) The half divergence angles ( $\theta_x$ : the dotted lines;  $\theta_y$ : the solid lines) of the  $y$ -polarized mode as a function of wavelength for various  $d_2/\Lambda$ .

$y$ -polarized mode. By applying Gaussian fitting to the normalized intensity, the mode field widths and the half divergence angles can be calculated. Fig. 5 shows the mode field widths and the half divergence angle for the two directions of the  $y$ -polarized modes as functions of wavelength for various  $d_2/\Lambda$  ratios. As expected, the mode becomes more confined for increased  $d_2/\Lambda$  ratio and, hence, displays a relatively smaller mode field width. On the contrary, the half divergence angle increases as the  $d_2/\Lambda$  ratio is increased. The effects of varying  $d_2/\Lambda$  on the mode width and divergence angle along the  $x$  direction (i.e.,  $w_x$

and  $\theta_x$ ) are significantly bigger than that along the  $y$  direction ( $w_y$  and  $\theta_y$ ).

### III. CONCLUSION

A highly birefringent PCF [4] is successfully modeled and analyzed by using a full-vector FEM. The calculated birefringence is in good agreement with the measurements reported previously in the literature. The birefringence may be further enhanced by increasing the size to pitch ratio for the bigger holes. The GVDs of the two polarization modes are significantly different, especially at longer wavelength. The mode field distribution has approximately an elliptical shape with the width of the major axis significant bigger than that of the minor axis. The mode field area increases from  $(w_x : w_y) = 2.02\mu\text{m} : 2.94\mu\text{m}$  at 1000 nm and to  $2.19\mu\text{m} : 3.4\mu\text{m}$  at 1500 nm. The half divergence angle is, however, significantly bigger along the minor axis than in the major axis and increased from  $(\theta_x : \theta_y) = 0.21\text{rad} : 0.31\text{rad}$  to  $0.28\text{rad} : 0.41\text{rad}$ . The mode field widths and the divergence angles can be adjusted by varying the parameters of the PCF.

### REFERENCES

- [1] T. A. Birks, J. C. Knight, and P. S. J. Russell, "Endlessly single-mode photonic crystal fiber," *Opt. Lett.*, vol. 22, pp. 961–963, July 1997.
- [2] J. K. Ranka, R. S. Windeler, and A. J. Stenz, "Optical properties of high-delta air-silica microstructure optical fibers," *Opt. Lett.*, vol. 25, pp. 796–798, June 2000.
- [3] J. C. Knight, J. Arriaga, T. A. Birks, A. Ortigosa-Blanch, W. J. Wadsworth, and P. S. J. Russell, "Anomalous dispersion in photonic crystal fiber," *IEEE Photon. Technol. Lett.*, vol. 12, pp. 807–809, July 2000.
- [4] A. Ortigosa-Blanch, J. C. Knight, W. J. Wadsworth, J. Arriaga, B. J. Mangan, T. A. Birks, and P. S. J. Russell, "Highly birefringent photonic crystal fibers," *Opt. Lett.*, vol. 25, pp. 1325–1327, Sept. 2000.
- [5] K. Suzuki, H. Kubota, S. Kawanishi, M. Tanaka, and M. Fujita, "High-speed bi-directional polarization division multiplexed optical transmission in ultra low-loss (1.3 dB/km) polarization-maintaining photonic crystal fiber," *Electron. Lett.*, vol. 37, pp. 1399–1401, Nov. 2001.
- [6] T. P. Hansen, J. Broeng, S. E. B. Libori, E. Knuders, A. Bjarklev, J. R. Jensen, and H. Simonsen, "Highly birefringent index-guiding photonic crystal fibers," *IEEE Photon. Technol. Lett.*, vol. 13, pp. 588–590, June 2001.
- [7] J. Noda, K. Okamoto, and Y. Sasaki, "Polarization-maintaining fibers and their applications," *J. Lightwave Technol.*, vol. 4, pp. 1071–1089, Aug. 1986.
- [8] B. M. Dillon and J. P. Webb, "A comparison of formulations for the vector finite element analysis of waveguide," *IEEE Trans. Microwave Theory Tech.*, vol. 42, pp. 308–316, Feb. 1994.
- [9] A. Cucinotta, S. Selleri, L. Vincetti, and M. Zoboli, "Holey fiber analysis through the finite element method," *IEEE Photon. Technol. Lett.*, vol. 14, pp. 1530–1532, Nov. 2002.
- [10] N. A. Mortensen, J. R. Folken, P. M. W. Skovgaard, and J. Broeng, "Numerical aperture of single-mode photonic crystal fibers," *IEEE Photon. Technol. Lett.*, vol. 14, pp. 1094–1096, Aug. 2002.